SF2A 2013
L. Cambrésy, F. Martins, E. Nuss and A. Palacios (eds)

MEASUREMENT OF THE THERMAL SUNYAEV-ZEL'DOVICH ANGULAR POWER SPECTRUM WITH PLANCK.

G. Hurier[1] and The Planck Collaboration

Abstract. The Planck experiment allows us to construct the first all-sky map of the thermal Sunyaev-Zeldovich (tSZ) effect by applying dedicated component separation algorithms to the 100 to 857 GHz frequency channel maps. These maps show a clear galaxy cluster tSZ signal that is well matched with blindly detected clusters in the Planck SZ catalogue. To characterize the signal in the tSZ map we have computed its angular power spectrum. We have carefully modeled and subtracted the foreground contaminant, mainly the diffuse thermal dust emission and Cosmic Infrared Background (CIB). Finally, we use the tSZ power spectrum to obtain constraints on cosmological parameters.

Keywords: cosmological parameters, large-scale structure of Universe, Galaxies: clusters: general

1 Introduction

The thermal Sunyaev-Zeldovich (tSZ) effect (Sunyaev & Zeldovich 1972), produced by the inverse Compton scattering of CMB photons by hot electrons along the line of sight, has proved to be a major tool to the study of the physics of clusters of galaxies as well as structure formation in the Universe. In particular, tSZ-selected catalogues of clusters of galaxies have been provided by various experiments including the *Planck* satellite (Planck Collaboration VIII 2011; Planck Collaboration XXIX 2013), the Atacama Cosmology Telescope (ACT, Hasselfield et al. 2013) and the South Pole Telescope (SPT, Reichardt et al. 2013). From these catalogues, and their associated sky surveys, a wealth of studies have been performed both on the physics of clusters of galaxies (Planck Collaboration XII 2011; Planck Collaboration XI 2011; Planck Collaboration X 2011) and on their cosmological interpretation (Planck Collaboration XX 2013; Benson et al. 2013; Das et al. 2013; Wilson et al. 2012; Mak & Pierpaoli 2012).

To date, indirect measurements of the tSZ power spectrum are only available from high resolution CMB oriented experiments like ACT (Sievers et al. 2013) and SPT (Reichardt et al. 2012). In these studies, constraints on the amplitude of tSZ power spectrum at $\ell = 3000$ are obtained by fitting a tSZ template in addition to other components (i.e., CMB, radio and infrared point-source and clustered Cosmic Infrared Background (CIB)) to the measured total power spectrum.

Thanks to its all sky coverage and unprecedented wide frequency range, *Planck* has the unique capability to produce an all-sky Compton parameter (y) map and an accurate measurement of the tSZ power spectrum at intermediate and large angular scales, for which the tSZ fluctuations are almost insensitive to the cluster core physics.

2 Planck Data

This paper is based on the first 15.5 month survey mission corresponding to two full-sky surveys. We refer to Planck Collaboration II (2013) and Planck Collaboration VI (2013) for the generic scheme of Time Ordered Information (TOI) processing and map-making, as well as for the technical characteristics of the *Planck* frequency maps. The *Planck* channel maps are provided in `HEALPix` (Górski et al. 2005) $N_{\rm side} = 2048$ at full resolution. An error map is associated with each channel map and is obtained from the difference of the first half and second half of the survey rings for a given pointing position of the satellite spin axis. The resulting maps, called null maps, are mainly free from astrophysical emission and they are a good representation of the statistical instrumental noise. Null maps have also been used to estimate the noise in the final Compton parameter maps. Here we approximate the *Planck* beams by effective circular Gaussians (Planck Collaboration IV 2013; Planck Collaboration VII 2013). Although tests have been performed using both LFI and HFI channel maps, the work presented here will refer mainly to results using the HFI data only.

[1] Institut d'Astrophysique Spatiale, CNRS (UMR8617) Universit Paris-Sud 11, Btiment 121, Orsay, France

3 The tSZ effect

The thermal SZ Compton parameter in a given direction, $\vec{n}$, is

$$y(\vec{n}) = \int n_e \frac{K_B T_e}{m_e c^2} \sigma_T \, \mathrm{d}s \tag{3.1}$$

where ds is the distance along the line-of-sight, $\vec{n}$, and n_e and T_e are the electron number density and temperature, respectively.

In units of CMB temperature the contribution of the tSZ effect to the *Planck* maps for a given observation frequency ν is

$$\frac{\Delta T}{T_{\rm CMB}} = g(\nu)\, y. \tag{3.2}$$

Neglecting relativistic corrections we have $g(\nu) = \left(x \coth(\frac{x}{2}) - 4\right)$, with $x = h\nu/(k_B T_{\rm CMB})$.

4 tSZ power spectrum

Decomposing the map in spherical harmonics we obtain

$$y(\vec{n}) = \sum_{\ell m} y_{\ell m}\, Y_{\ell m}\,(\vec{n}), \tag{4.1}$$

Thus, the angular power spectrum of the Compton parameter map is

$$C_\ell^{\rm tSZ} = \frac{1}{2\,\ell + 1} \sum_m y_{\ell m} y^*_{\ell m}. \tag{4.2}$$

Note that $C_\ell^{\rm tSZ}$ is an a-dimensional quantity as y.

To model the tSZ power spectrum we consider a two halo model to account for intra-halo and inter-halo correlations

$$C_\ell^{\rm SZ} = C_\ell^{\rm 1halo} + C_\ell^{\rm 2halos}. \tag{4.3}$$

In the case of the tSZ emission the inter-halo term can neglected with respect to the 1-halo term. The 1 halo term, also known as the Poissonian contribution, can be computed by summing the square of the Fourier transform of the projected SZ profile, weighted by the number density of clusters of a given mass and redshift (Komatsu & Seljak 2002):

$$C_\ell^{\rm 1halo} = \int_0^{z_{\rm max}} dz \frac{dV_c}{dz d\Omega} \int_{M_{\rm min}}^{M_{\rm max}} dM \frac{dn(M,z)}{dM} \left|\tilde{y}_\ell(M,z)\right|^2, \tag{4.4}$$

where $dV_c/(dz d\Omega)$ is the comoving volume per unit redshift and solid angle and $n(M,z)dM\, dV_c/(dz d\Omega)$ is the probability of having a galaxy cluster of mass M at a redshift z in the direction $d\Omega$. The quantity $\tilde{y}_\ell = \tilde{y}_\ell(M,z)$ is the 2D Fourier transform on the sphere of the 3D radial profile of the Compton y-parameter of individual clusters,

$$\tilde{y}_\ell(M,z) = \frac{4\pi r_s}{\ell_s^2} \left(\frac{\sigma_T}{m_e c^2}\right) \int_0^\infty dx\, x^2 P_e(M,z,x) \frac{\sin(\ell x/\ell_s)}{\ell x/\ell_s} \tag{4.5}$$

where $x = r/r_s$, $\ell_s = D_A(z)/r_s$, r_s is the scale radius of the 3D pressure profile, $D_A(z)$ is the angular diameter distance to redshift z and P_e is the electron pressure profile.

5 Reconstruction of an all-sky tSZ map

The contribution of the tSZ effect in the *Planck* frequency maps is subdominant with respect to the CMB and other foreground emissions. Furthermore, the tSZ effect from galaxy clusters is spatially localized and leads to a highly non-Gaussian signal with respect to that from the CMB. CMB-oriented component-separation methods (Planck Collaboration XII 2013) are not optimized to recover the tSZ signal. We therefore need to use specifically tailored component separation algorithms that are able to reconstruct the tSZ signal from the *Planck* frequency channel maps. These optimized all-sky component separation techniques rely on the spatial localization of the different astrophysical components and on their

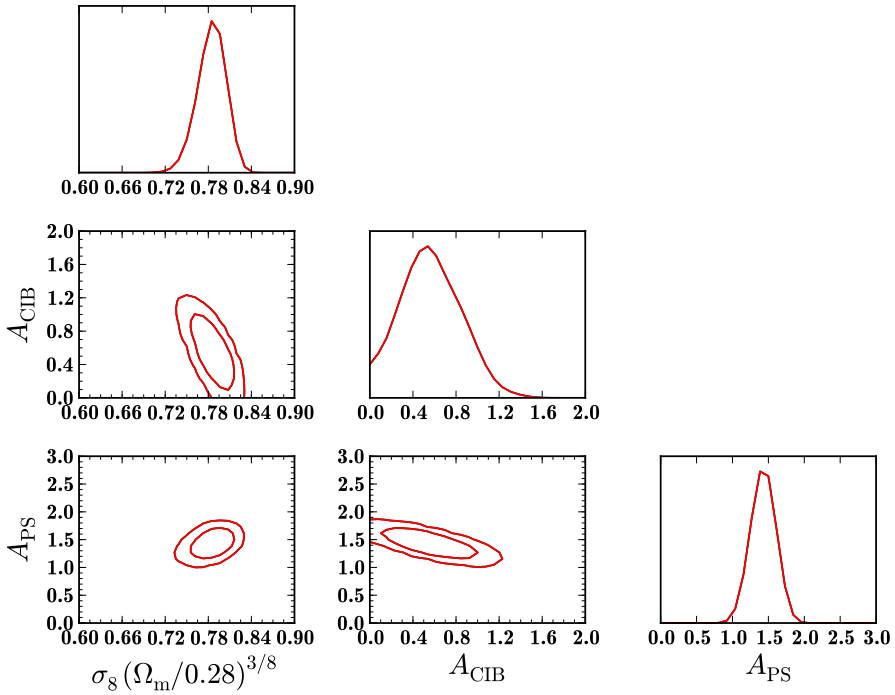

Fig. 1. 2D and 1D likelihood distributions for the combination of cosmological parameters $\sigma_8(\Omega_{\rm m}/0.28)^{3.2/8.1}$, and for the foreground parameters $A_{\rm CIB}$ and $A_{\rm PS}$. We show the 68% and 95.4% C.L. contours here.

spectral diversity to separate them. We present,in the following, the results of two algorithms, MILCA (Modified Internal Linear Combination Algorithm, Hurier et al. 2010) and NILC (Needlet Iindependent Linear Combination, Remazeilles et al. 2011). Both are based on the well known Internal Linear Combination (ILC) approach that searches for the linear combination of the input maps that minimizes the variance of the final reconstructed map under the constraint of offering unit gain to the component of interest (here the tSZ effect, whose frequency dependence is known). Both have been extensively tested on simulated *Planck* data.

6 Power spectrum analysis

As a measure of structure growth, the tSZ power spectrum can provide independent constraints on cosmological parameters and potentially improve their precision. As shown by Komatsu & Seljak (2002), the power spectrum of the tSZ effect is highly sensitive to the normalization of the matter power spectrum, commonly parameterized by the rms of the $z = 0$ mass distribution on $8\,h^{-1}$ Mpc scales, σ_8 (Komatsu & Seljak 2002), and to the total amount of matter $\Omega_{\rm m}$.

Cosmological constraints are obtained from a fit of the NILC F/L cross-power spectrum, for the 50% mask, assuming a three-component model: tSZ; clustered CIB; and radio and infrared point sources. For $\ell > 60$, we can reasonably neglect the Galactic dust contamination. For $\ell > 1411$ the total signal in the tSZ map is dominated by noise. We thus restrict our analysis to the multipole range $60 < \ell < 1411$. The measured power spectrum, $C_\ell^{\rm m}$, is modelled as follows:

$$C_\ell^{\rm m} = C_\ell^{\rm tSZ}(\Omega_{\rm m}, \sigma_8) + A_{\rm CIB}\, C_\ell^{\rm CIB} + A_{\rm PS}\, (C_\ell^{\rm IR} + C_\ell^{\rm Rad}). \quad (6.1)$$

Here $C_\ell^{\rm tSZ}(\Omega_{\rm m}, \sigma_8)$ is the tSZ power spectrum, $C_\ell^{\rm CIB}$ is the clustered CIB power spectrum and $C_\ell^{\rm IR}$ and $C_\ell^{\rm Rad}$ are the infrared and radio source power spectra, respectively.

The tSZ spectrum is computed using the halo model, the Tinker et al. (2008) mass function and the Arnaud et al. (2010) universal pressure profile. In particular, we use the numerical implementation presented in Taburet et al. (2009, 2010, 2011) and integrate in redshift from 0 to 3 and in mass from 10^{13} to 5×10^{15} $M_\odot$. Our model allows us to compute the tSZ power spectrum at the largest angular scales.

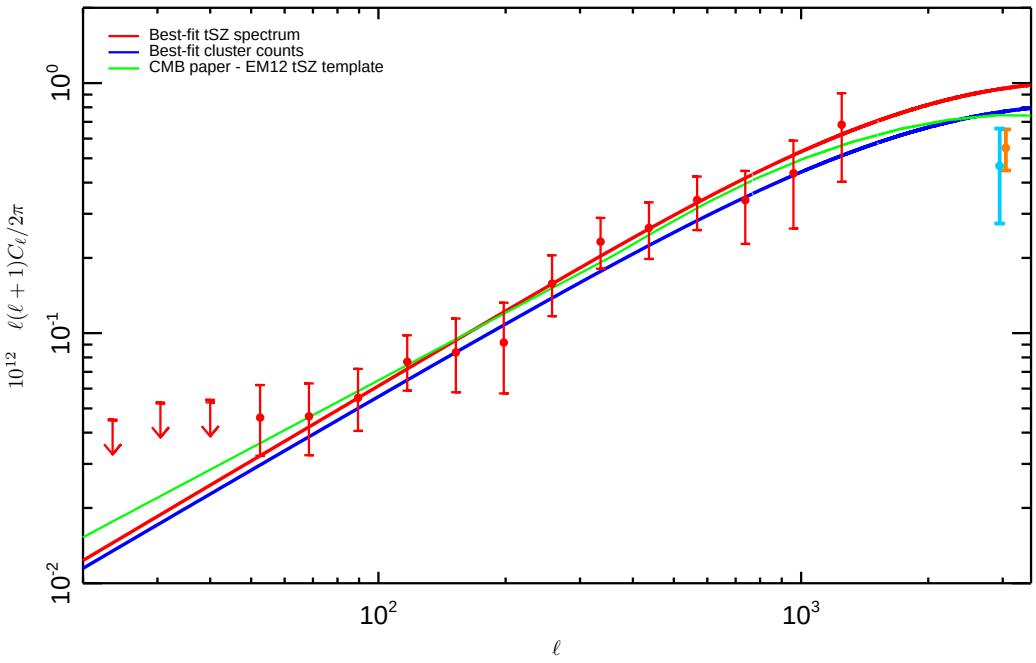

Fig. 2. Marginalized bandpowers of the *Planck* tSZ power spectrum with total (statistical plus foreground) uncertainties (red points). The red solid line represents the best-fit tSZ power spectrum model. We also show as a blue solid line the best-ft tSZ power-spectrum obtained from the analysis of cluster number counts (Planck Collaboration XX 2013). The tSZ power spectrum template used in the CMB cosmological analysis (Planck Collaboration XV 2013; Planck Collaboration XVI 2013) is presented as a green solid line.

We allow for a variation of the normalization amplitudes for the clustered CIB, $A_{\rm CIB}$ and for the point sources, $A_{\rm PS}$, with Gaussian priors centred on one with standard deviation 0.5.

We assume a Gaussian approximation for the likelihood function. Best-fit values and uncertainties are obtained using an adapted version of the `Cosmo-MC` algorithm (Lewis & Bridle 2002). Only σ_8 and $\Omega_{\rm m}$ are allowed to vary here. All other cosmological parameters are fixed to their best-fit values as obtained in Table 2 of Planck Collaboration XVI (2013). The normalization amplitudes $A_{\rm CIB}$ and $A_{\rm PS}$, considered as nuisance parameters, are allowed to vary between 0 and 3. For the range of multipoles considered here, the tSZ angular power spectrum varies like $C_\ell \propto \sigma_8^{8.1}\Omega_{\rm m}^{3.2}$. The results are thus presented in terms of this parameter combination.

Figure 1 presents the 2D and 1D likelihood distributions for the cosmological parameter combination $\sigma_8\Omega_{\rm m}^{3.2/8.1}$, and for the foreground nuisance parameters. The best-fit values and error bars for each parameter are given by $\sigma_8(\Omega_{\rm m}/0.28)^{3.2/8.1} = 0.784 \pm 0.016$, $\sigma_8 = 0.74 \pm 0.06$, $\Omega_{\rm m} = 0.33 \pm 0.06$, $A_{\rm CIB} = 0.55 \pm 0.26$ and $A_{\rm PS} = 0.14 \pm 0.13$. It is worth noting that these values are obtained in a specific framework: all other cosmological parameters fixed and a fiducial fixed model for the signals. Opening up the possibility for relaxing this framework is likely to weaken the constraints.

The red points in Fig. 2 correspond to the marginalized *Planck* tSZ power spectrum (from the `NILC` F/L cross-power spectrum), compared to the best-fit theoretical model presented above (solid red line). Foreground uncertainties are derived from the likelihood curves of the nuisance parameters and added in quadrature to the statistical uncertainties, providing the total errors plotted here. In the range ℓ=60–1411, the *Planck* tSZ power spectrum can be approximated by a power law of the form

$$\ell(\ell+1)C_\ell/2\pi = (1.0 \pm 0.2)\ \ell^{(0.912\pm0.031)}\ 10^{-15}.$$

The measured tSZ power-spectrum is in remarkable agreement with the tSZ power-spectrum (blue solid line) computed using cluster count best-fit parameters (Planck Collaboration XX 2013).

7 Conclusion

Because of its wide frequency coverage from 30 to 857 GHz, the *Planck* satellite mission is particularly well suited for the measurement of the thermal Sunyaev-Zeldovich effect.

We have produced the first measurement of the SZ power spectrum on large angular scales ranging from $0.17^\circ \lesssim \theta \lesssim 3.0^\circ$. In this range, the tSZ power spectrum is almost insensitive to the physics of cluster cores. The detected tSZ signal likely arises from the contribution of warm and hot diffuse gas distributed within groups and clusters, sampling the whole halo mass function, as well as within the larger scale filamentary structures.

We have modelled the tSZ power spectrum via a halo-model analytical approach, in order investigate its dependence in terms of σ_8 and Ω_m and to test it against the measured *Planck* tSZ power spectrum.

The observed consistency between constraints derived from the cluster number counts in Planck Collaboration XX (2013) and from the present work seems to provide a coherent view of the gas content in halos and in larger scale structures. As such, this *Planck* tSZ measurement constitutes the first step towards building a coherent understanding of the integrated tSZ effect due to cosmic structure on all scales and density contrasts.

The development of *Planck* has been supported by: ESA; CNES and CNRS/INSU-IN2P3-INP (France); ASI, CNR, and INAF (Italy); NASA and DoE (USA); STFC and UKSA (UK); CSIC, MICINN, JA and RES (Spain); Tekes, AoF and CSC (Finland); DLR and MPG (Germany); CSA (Canada); DTU Space (Denmark); SER/SSO (Switzerland); RCN (Norway); SFI (Ireland); FCT/MCTES (Portugal); and PRACE (EU). A description of the *Planck* Collaboration and a list of its members, including the technical or scientific activities in which they have been involved, can be found at http://www.sciops.esa.int/index.php?project=Planck&page=Planck_Collaboration. We acknowledge the use of the HEALPix software.

References

Arnaud, M., Pratt, G. W., Piffaretti, R., et al. 2010, A&A, 517, A92

Benson, B. A., de Haan, T., Dudley, J. P., et al. 2013, The Astrophysical Journal, 763, 147

Das, S., Louis, T., Nolta, M. R., et al. 2013, eprint arXiv, 1301, 1037

Górski, K. M., Hivon, E., Banday, A. J., et al. 2005, ApJ, 622, 759

Hasselfield, M., Hilton, M., Marriage, T. A., et al. 2013, eprint arXiv, 1301, 816, 32 pages, 21 figures

Hurier, G., Hildebrandt, S. R., & Macias-Perez, J. F. 2010, ArXiv e-prints

Komatsu, E. & Seljak, U. 2002, Monthly Notice of the Royal Astronomical Society, 336, 1256

Komatsu, E. & Seljak, U. 2002, MNRAS, 336, 1256

Lewis, A. & Bridle, S. 2002, Phys. Rev. D, 66, 103511

Mak, D. S. Y. & Pierpaoli, E. 2012, Physical Review D, 86, 123520

Planck Collaboration II. 2013, Submitted to A&A

Planck Collaboration IV. 2013, Submitted to A&A

Planck Collaboration VI. 2013, Submitted to A&A

Planck Collaboration VII. 2013, Submitted to A&A

Planck Collaboration VIII. 2011, A&A, 536, A8

Planck Collaboration X. 2011, A&A, 536, A10

Planck Collaboration XI. 2011, A&A, 536, A11

Planck Collaboration XII. 2011, A&A, 536, A12

Planck Collaboration XII. 2013, Submitted to A&A

Planck Collaboration XV. 2013, Submitted to A&A

Planck Collaboration XVI. 2013, Submitted to A&A

Planck Collaboration XX. 2013, Submitted to A&A

Planck Collaboration XXIX. 2013, Submitted to A&A

Reichardt, C. L., Shaw, L., Zahn, O., et al. 2012, ApJ, 755, 70

Reichardt, C. L., Stalder, B., Bleem, L. E., et al. 2013, The Astrophysical Journal, 763, 127

Remazeilles, M., Delabrouille, J., & Cardoso, J.-F. 2011, MNRAS, 410, 2481

Sievers, J. L., Hlozek, R. A., Nolta, M. R., et al. 2013, eprint arXiv, 1301, 824

Sunyaev, R. A. & Zeldovich, Y. B. 1972, Comments on Astrophysics and Space Physics, 4, 173

Taburet, N., Aghanim, N., Douspis, M., & Langer, M. 2009, mnras, 392, 1153

Taburet, N., Douspis, M., & Aghanim, N. 2010, mnras, 404, 1197

Taburet, N., Hernández-Monteagudo, C., Aghanim, N., Douspis, M., & Sunyaev, R. A. 2011, MNRAS, 418, 2207

Tinker, J., Kravtsov, A. V., Klypin, A., et al. 2008, The Astrophysical Journal, 688, 709

Wilson, M. J., Sherwin, B. D., Hill, J. C., et al. 2012, Physical Review D, 86, 122005